


RESEARCH

Open Access



Growth and physiological impairments in Fe-starved alfalfa are associated with the downregulation of Fe and S transporters along with redox imbalance

Md Atikur Rahman¹, Md Bulbul Ahmed², Fahad Alotaibi^{3,4}, Khaled D. Alotaibi^{3,5}, Noura Ziadi⁵, Ki-Won Lee¹ and Ahmad Humayan Kabir^{6*} 

Abstract

Background: Iron (Fe) is an essential plant nutrient. Its deficiency is a major constraint in crop production systems, affecting crop yield and quality. It is therefore important to elucidate the responses and adaptive mechanisms underlying Fe-deficiency symptoms in alfalfa.

Materials and methods: The experiment was carried out on 12-day-old alfalfa plants grown in hydroponics under Fe-sufficient and Fe-deficient conditions.

Results: The Fe-starved alfalfa showed decreased plant biomass, chlorophyll score, PSII efficiency, and photosynthesis performance index in young leaves under low Fe. Further, Fe shortage reduced the Fe, Zn, S and Ca concentration in root and shoot of alfalfa accompanied by the marked decrease of *MsIRT1*, *MsZIP*, *MsSULTR1;1*, *MsSULTR1;2* and *MsSULTR1;3* transcripts in root and shoot. It indicates that retardation caused by Fe-deficiency was also associated with the status of other elements, especially the reduced Fe and S may be coordinately attributed to the photosynthetic damages in Fe-deficient alfalfa. The ferric chelate reductase activity accompanied by the expression of *MsFRO1* in roots showed no substantial changes, indicating the possible involvement of this Strategy I response in Fe-deficient alfalfa. However, the proton extrusion and expression of *MsHAI1* were significantly induced following Fe-deficiency. In silico analysis further suggested their subcellular localization in the plasma membrane. Also, the interactome map suggested the partnership of *MsFRO1* with plasma membrane H⁺-ATPase, transcription factor *bHLH47*, and nitrate reductase genes, while *MsHAI1* partners include ferric reductase-like transmembrane component, plasma membrane ATPase, vacuolar-type H-pyrophosphatase, and general regulatory factor 2. In this study, SOD and APX enzymes showed a substantial increase in roots but unable to restore the oxidative damages in Fe-starved alfalfa.

Conclusion: These findings promote further studies for the improvement of Fe-starved alfalfa or legumes through breeding or transgenic approaches.

Keywords: Fe deprivation, Alfalfa, FCR activity, Transporter genes, Proton extrusion

Introduction

Iron (Fe) deficiency in plants is a common issue in agricultural systems, as this adversely affects the growth and development of all plant types and species. The Fe availability in soil system is influenced by several factors, including soil pH, texture, organic matter, cation

*Correspondence: ahmad.kabir@ru.ac.bd

⁶ Molecular Plant Physiology Laboratory, Department of Botany, University of Rajshahi, Rajshahi 6205, Bangladesh

Full list of author information is available at the end of the article

exchange capacity and soil minerals [1, 2]. The Fe-deficiency is more common in alkaline and calcareous soils where added Fe rapidly gets precipitated in insoluble forms and becomes unavailable for plants. The Fe functions in plants include its involvement in many physiological and biochemical processes, such as photosynthesis, respiration, and protein formation [3]. Photosystem II (PS-II) also loses its efficiency due to low photosynthetic electron sources to Fe-depleted plants [4]. As a result, Fe deficiency causes stunted root, leaf chlorosis, and poor maturation in plants [1, 5]. The production and secretion of chemicals that aid in efficient Fe uptake in alfalfa is critical, although little is known about it [6]. Particularly, the secretion of phenolics by the roots of a dicot species in response to Fe deficiency enhances plant Fe nutrition by increasing apoplastic Fe reutilization and thereby boosting Fe nutrition in the shoot [7]. Thus, the consequences of Fe-deficiency affecting the mineral nutrition and growth of plants are crucial for plant improvement.

Via the root system, plants use two different Fe absorption methods. Fe is acquired by rhizosphere-based reduction mechanisms in a Strategy-I plant. The operation of root ferric chelate reductase (FCR) aids ferric to ferrous ion conversion, allowing existing Fe in the plasma membrane to be used [8]. In many dicot plant species, FCR activity and upregulation of its candidate gene (*FRO*) have been reported to confer Fe-deficiency tolerance [1, 9]. Furthermore, causing acidification in the rhizosphere by proton (H⁺) extrusion boosts Fe mobilization [10]. Several Strategy-I plants have been found to have genes linked to this function, such as Arabidopsis' *AtAHA7* [11]. Although there are few disagreements about the function of phenolics in increasing Fe availability in the rhizosphere, there are a few reports that suggest phenolics can influence the microbial community for Fe incensement in plants [12]. Along with the mechanisms involved with Fe availability and mobilization in the rhizosphere, some transporter genes are also prominently associated with Fe uptake in plants. It is also clear that interactions of Fe with other mineral elements, such as Zn, S, and Ca, in plants suffering from Fe deficiency, are frequently related to the overall response of plants. The *IRT1* gene (Fe-regulated transporter protein) is the most common Fe transporter found in plants, including tomato [13], field peas1, and Arabidopsis [14, 15]. In plants, Fe and Zn homeostasis are mutually beneficial. In Fe-deficient origin, the IRT gene families are expressed in epidermal cells to mediate Zn transporter [14, 15]. In Fe-deficient plants, Nramp1 (natural resistance-associated macrophage protein) also plays a role in Fe²⁺ transporter [16, 17]. Several ZIP proteins were found to be influenced by Fe/Zn deficiency [18]. Since most active Fe in Fe-S protein clusters is linked to S in the chloroplast and

cytochrome complex, the relationship between Fe and S is crucial in the response to Fe deficiency [19]. Several members of the *SULTR* gene family mediate the uptake of S in the root plasmalemma and cell cells [20, 21]. Calcium itself is a nutrient element but also serves as the second message in response to mineral deficiency [22, 23]. The Fe-deficiency contributes to elevated reactive oxygen species (ROS) molecular that causes oxidative damages in plant cells [24]. However, several antioxidant metabolites and enzymes are often in action to regulate the redox balance, although which is mostly seen in Fe-efficient plant species/cultivar [25]. However, high antioxidant properties are mostly seen in sensitive varieties specific to particular stress [26]. Moreover, antioxidant activities in response to stress varied in plant species, tissues, and subcellular localization [27]. The differential response of the antioxidant system in response to Fe deficiency varies among the genotypes/species.

Alfalfa (*Medicago sativa* L.) is a legume that is primarily used as a hay crop because of its high nutritional value, but it can also improve soil fertility by nitrogen fixation. However, no research has been done on the responses and characterization of alfalfa Fe-acquisition genes in response to Fe deficiency. As a result, we looked into how Fe deficiency affects alfalfa plant growth and development. Along with the morpho-physiological evidence, a broad range of cellular and molecular evidence figured out the mechanistic basis of Fe-deficiency-induced retardation in alfalfa.

Materials and methods

Plant cultivation system

Alfalfa (cv. Vernal) seeds were surface-sterilized for 3 min with 70% ethyl alcohol, then washed with distilled water. The seeds were then germinated on a tray for 2 days at room temperature before being transferred to solution culture (pH 6.0) in a 5 L plastic pot, as mentioned previously [28, 29]. Fe-EDTA was added to alfalfa seedlings at two separate concentrations: 25 μ M Fe-EDTA (+Fe) and 1.0 μ M Fe-EDTA (-Fe). The pH of the solution was fixed to 6.0. There were nine plants per pot for each treatment. The seedlings were grown in a growth cabinet with a 14/10 h light/dark photoperiod (550–560 mol s⁻¹ per A). After 12 days, the plants were harvested for study.

Morphological and photosynthesis features

The length of the longest root and shoot was measured with a digital caliper. After drying for 3 days at 80 °C in an electric oven, the dry weight of the root and shoot was determined. The SPAD meter was used to measure the chlorophyll content of young leaves (Minolta, Japan). Furthermore, photosynthesis biophysics by chlorophyll fluorescence kinetic (OJIP) of young leaves

held for 1 h at dark using FP 100, such as Fv/Fm (quantum efficiency of photosystem II), Pi_ABS (photosynthesis output index), and Mo (approximated initial slope in ms^{-1} of the fluorescent transient) (Photon Systems Instruments, Czech Republic).

Analysis of elemental concentration

Surface elements were removed from alfalfa root samples using Milli-Q water. Roots were then washed 2–3 times in Milli-Q water and incubated at 4 °C with 10 mM MES) and then with 10 mM MES+1 mM EDTA solutions. After surface cleaning, the root and shoot were placed in a falcon tube with the lid open for 3 days to dry at 70 °C. Following that, dried samples were digested with $\text{HNO}_3/\text{HClO}_4$ (3:1 v/v) and volume increased to 10 ml. The solution was then subjected to inductively coupled plasma mass spectroscopy for elemental analysis based on standard curves (ICP-MS, Agilent 7700, USA).

Analysis of stress indicators

The cell death rate was tested by Evans blue [30]. The entire fresh root and shoot were quickly transferred to a tube containing 2 mL of Evan's blue mixture, and 15 min was allowed to pass. In 1 ml of 80 percent ethanol solution, the suspension was dried for 10 min. The tubes containing the solutions were incubated for 15 min at 50 degrees Celsius in a water bath before being centrifuged for 10 min at 12,000 rpm. At 600 nm, the supernatant's absorbance was determined. Finally, using the sample-fresh weight, the percentage of cell death was calculated.

A conductivity meter was used to calculate the final effects of loss of cell membrane integrity in both root and shoot tissues [31]. Deionized water was used to wash the root and shoot surface components. Fresh specimens were then placed in a 20 mL deionized water beaker and held at 25 °C for 2 h. The electrical conductivity (EC1) of the solution was then determined. The samples were then heated in a water bath at 95 °C for 20 min to ensure optimal electrolyte release, then cooled to 25 °C. The final EC was then registered and calculated as follows (%): $(\text{EC1}/\text{EC2}) \text{ EC} = (\text{EC1}/\text{EC2}) \text{ EC} = (\text{EC1}/\text{EC2}) \text{ EC} = (\text{EC1}/\text{EC2})$.

H_2O_2 accumulation was assessed using 0.1 percent trichloroacetic acid (TCA) from the fresh root and shoot samples, as previously described [32]. The extracted liquid was spun at 10,000 rpm for 15 min to separate the aqueous portion. The top aqueous segment was supplemented with 10 mM potassium phosphate (pH 7.0), 1 M KI, and held in the dark for 1 h to allow for reaction. Finally, the mixture's optical density was measured at 390 nm.

The activity of Fe chelate reductase assay

The ferrozine assay was used to measure FCR root activity [9]. Briefly, 0.1 g root was washed clean with 0.2 mM CaSO_4 and Milli-Q water. After that, 1 ml of the assay mixture (100 mM Fe(III) EDTA, 0.10 mmol MES–NaOH (pH 5.5), 300 mM ferrozine) was added to the roots samples. The samples and blank tube (without the assay mixture) were held at 25 °C for 20 min in the dark. At 562 nm, aliquots were finally read. The ferrozine molar extinction coefficient was used to calculate the FCR activity.

Estimation of rhizosphere acidification

The secretions of H^+ from roots known as proton extrusion were tested with a titration method. Briefly, the pH of the cultivation medium was maintained by 0.1 M HCl or 0.1 M KOH. The H^+ efflux was measured after calculation [1].

Estimation of total phenolics

The concentration of total phenolics in roots was determined as previously mentioned [33]. In a nutshell, the root extract was combined with 80 percent Folin–Ciocalteu reagent and a 20% Na_2CO_3 solution. The solution's optical density was measured at 765 nm. The gallic acid calibration curve was used to determine the unknown sample concentration, which was expressed as mg of L^{-1} gallic acid g^{-1} extract (GAE).

The qRT-PCR analysis and bioinformatics analysis

Total RNA was extracted from root and leaf tissues following the high-quality RNeasy[®] plant mini kit (QIAGEN, Germany) protocol guidelines. Isolated RNA was then quantified by UV/Vis spectrophotometer (Avans Biotechnology Corporation, Taiwan). The quality and quantity of RNA were checked by Nanodrop Spectrophotometer. The first-strand cDNA was synthesized from 1 μg of total RNA using the cDNA synthesis kit (Bio-Rad, USA). The qPCR was run using Green Supermix in a CFX96 Real-Time system (Bio-Rad, USA) with gene-specific primers (Additional file 1: Table S1). The PCR program was set as follows: 95 °C for 3 min, followed by 40 cycles at 95 °C for 10 s, 60 °C for 30 s. The relative expression of genes was calculated by $\text{dd} - \Delta\text{Ct}$ method (Livak and Schmittgen, 2001) considered *MsActin* as an internal control.

NCBI Blast program was run to retrieve the mRNA and protein sequences of *MsFRO1* and *MsHAI*. The CELLO (<http://cello.life.nctu.edu.tw>) server predicted the subcellular localization of proteins [34]. The interactome map

was generated using the STRING server (<http://string-db.org>) visualized in Cytoscape [35].

Analysis of antioxidant enzymes

In a nutshell, the root and shoot of plants were homogenized separately in a mortar and pestle with 100 mM phosphate buffer (potassium phosphate, changed pH 7.0). The homogenate was centrifuged for 10 min at 8000 rpm to separate the transparent part for enzyme activity monitoring. To measure superoxide dismutase (SOD) activity, 100- μ L plant extract was mixed with 0.1 mM EDTA, 50 mM NaHCO_3 (pH 9.8), and 0.6 mM epinephrine, as well as the previously described protocol [36]. The adrenochrome confirmation was read at 475 min later. 0.1 mM EDTA, 50 mM potassium phosphate buffer with a fixed pH of 7.0, 0.1 mM H_2O_2 , and 0.5 mM ascorbic acid is used to combine 0.1 mL extract for ascorbate peroxidase (APX) activity [37]. Following that, the mixture's absorbance was measured at 290 nm, and the extinction coefficient ($2.8 \text{ mM}^{-1} \text{ cm}^{-1}$) was used to calculate the APX analysis. For CAT analysis, 100- μ L plant extract was mixed with 6% hydrogen peroxide and the absorbance of the solution was monitored at 240 nm in 30 s to 1 min break (extinguishing coefficient $0.036 \text{ mM}^{-1} \text{ cm}^{-1}$). In addition, a 100 μ L plant extract was mixed with 0.2 mol KP buffer (pH 7.0), 1 mM EDTA, 20 mM GSSG, and 0.2 mM NADPH. NADPH-oxidation at 340 nm decreased the GSSG and absorption that started the reaction. Finally, as previously stated [24], the GR activity was estimated using the extinction coefficient ($6.12 \text{ mM}^{-1} \text{ cm}^{-1}$).

Analysis of S-metabolites

We used a dual Waters 2489 detector to study the S-metabolites in roots using high-performance liquid

chromatography (HPLC) at 280 and 360 nm [28]. As gradient conditions, we used a C18 reverse-phase column with 100 percent acetonitrile as the mobile phase [28]. Until injection (20 l), the extracts and samples were diluted (100) and screened through 0.22 μ m Minisart Syringe Filters.

Statistical analysis

A randomized block design was used to perform experiments with three separate biological replications for each treatment. A t-test in Microsoft Excel 2007 was used to determine the significance of the +Fe and -Fe conditions. GraphPad Prism 6 was used to construct the graphic figures.

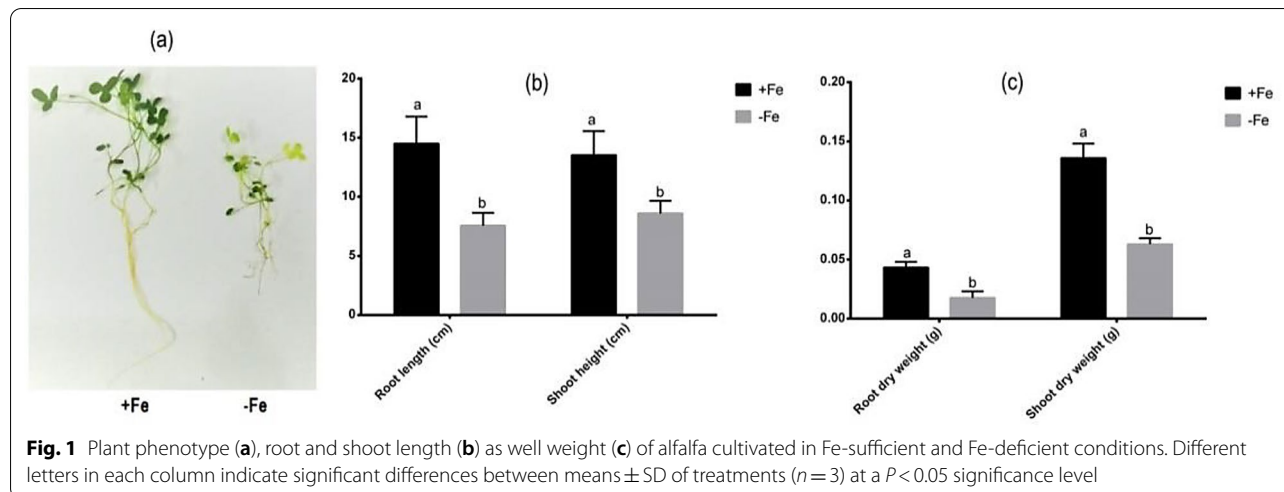
Results

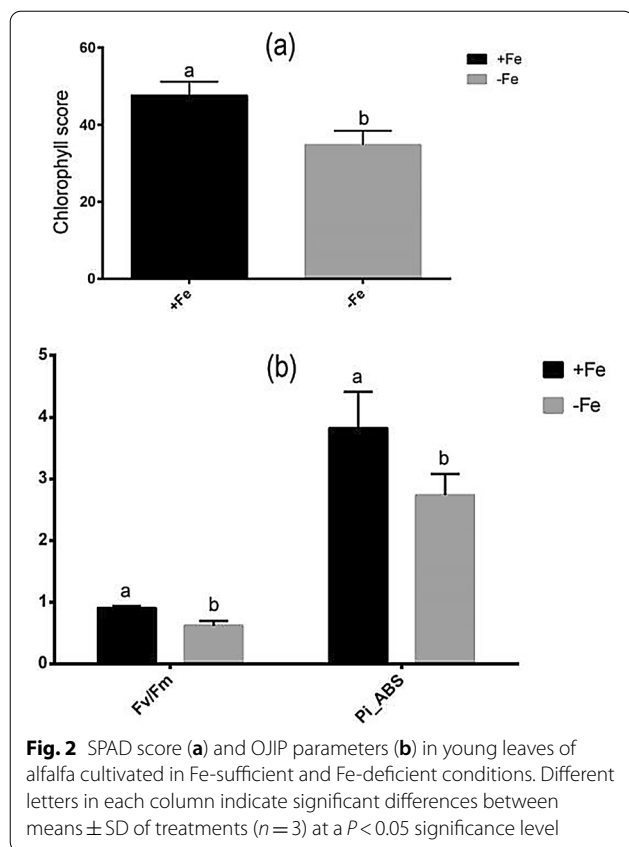
Plant growth and photosynthesis efficiency

The alfalfa plants showed distinct visual symptoms due to Fe-deficiency (Fig. 1a). Further, root length, root dry weight, shoot height and shoot dry weight were significantly decreased in Fe-deficient alfalfa in contrast to Fe-sufficient plants (Fig. 1a, b). In addition, chlorophyll score, Fv/Fm, and Pi_ABS values, indicating the status of photosynthesis, showed a significant declined in young leaves of alfalfa subjected to Fe-starvation with respect of Fe-adequate controls (Fig. 2).

Changes in stress indicators and Strategy I responses

We have analyzed electrolyte leakage, cell death %, and H_2O_2 concentration, known as stress indicators in plants, subjected to Fe-deficiency in alfalfa. We found that all of these parameters significantly increased in the root and shoot due to Fe-deprivation compared to the Fe-sufficient plants (Fig. 3a–c).





After Fe-deficiency, FCR activity in the roots showed no significant changes compared with Fe-sufficient controls (Fig. 3d). In contrast, H^+ extrusion in roots significantly increased in response to Fe-starvation relative to Fe-sufficient controls (Fig. 3e). However, the total phenolic concentration remained unchanged in the roots of alfalfa in response to Fe-shortage relative to controls (Fig. 3f).

Changes in elemental concentrations

Elemental analysis of Fe, Zn, S, and Ca was performed in order to see whether Fe-deficiency alters the concentration of Fe as well as other elements in alfalfa. Interestingly, not only the concentration of Fe but also Zn, S, and Ca showed a substantial decline in both the root and shoot of Fe-starved alfalfa relative to Fe-sufficient controls (Table 1).

Changes in the expression of Fe transporters

Our comprehensive qPCR analysis showed that *MsIRT1*, *MsZIP*, *MsSULTR1;1*, *MsSULTR1;2* and *MsSULTR1;3* transcripts showed a consistent decrease in the expression pattern both in root and shoot Fe-starved alfalfa compared to Fe-sufficient controls (Fig. 4a, c, d, e, f). However, the *MsNramp1* expression remained

unchanged in the root and shoot of alfalfa owing to Fe-shortage relative to controls (Fig. 4b).

Characterization of Strategy I genes

In roots, the *MsFRO1* gene was constitutively expressed subjected to Fe-starvation compared to Fe-sufficient plants (Fig. 5a). In contrast, the expression of the *MsHAI1* gene showed significant induction in the roots of alfalfa in response to Fe deprivation relative to controls (Fig. 5a). The Cello localization tool showed that *MsFRO1* and *MsHAI1* genes were predominantly localized in the plasma membrane (Fig. 5b). Interactome analysis showed that the *MsFRO1* gene was in close partnership with plasma membrane H^+ -ATPase, transcription factor *bHLH47* and nitrate reductase genes while *MsHAI1* partners include ferric reductase-like transmembrane component, plasma membrane ATPase, vacuolar-type H-pyrophosphatase, and general regulatory factor 2 (Fig. 5c).

Antioxidant efficiency

Activities of major antioxidant enzymes were assessed to determine how antioxidant defense counteracts the elevated ROS in alfalfa owing to Fe shortage. In this study, the CAT activity in root and shoot of alfalfa did not vary between Fe-sufficient and Fe-deficient conditions (Fig. 6a). Further, SOD and APX activities showed significant induction in the root, but these enzymes remained unchanged in shoot under Fe-shortage relative to Fe-sufficient controls (Fig. 6b, c). Finally, the activity of GR significantly declined in either root or shoot subjected to Fe-starvation in contrast to Fe-sufficient controls (Fig. 6d). Furthermore, HPLC results showed no significant changes in S-metabolites (glutathione, cysteine and methionine) in roots of alfalfa between Fe-sufficient and Fe-deficient conditions (Table 2).

Discussion

Plant growth and photosynthesis under Fe deficiency

While Fe deficiency harms plants, there is still a lack of clarity on how this nutritional stress affects alfalfa. The differential responses of alfalfa in response to Fe-deficiency were previously reported [38]. In this study, the induction of Fe deficiency in alfalfa resulted in a significant reduction in root and shoot characteristics in this study. Along with the visual leaf symptoms, the SPAD score dramatically dropped due to Fe starvation, suggesting the damages of photosynthesis efficiency and lack of Fe-containing enzymes associated with chlorophyll biosynthesis pathway in alfalfa leaves. The report of PSII status in alfalfa plants under Fe shortage is minimal. Our in-depth *Chl a* fluorescence analysis consistently showed the decrease in Fv/Fm value in leaves. It strongly

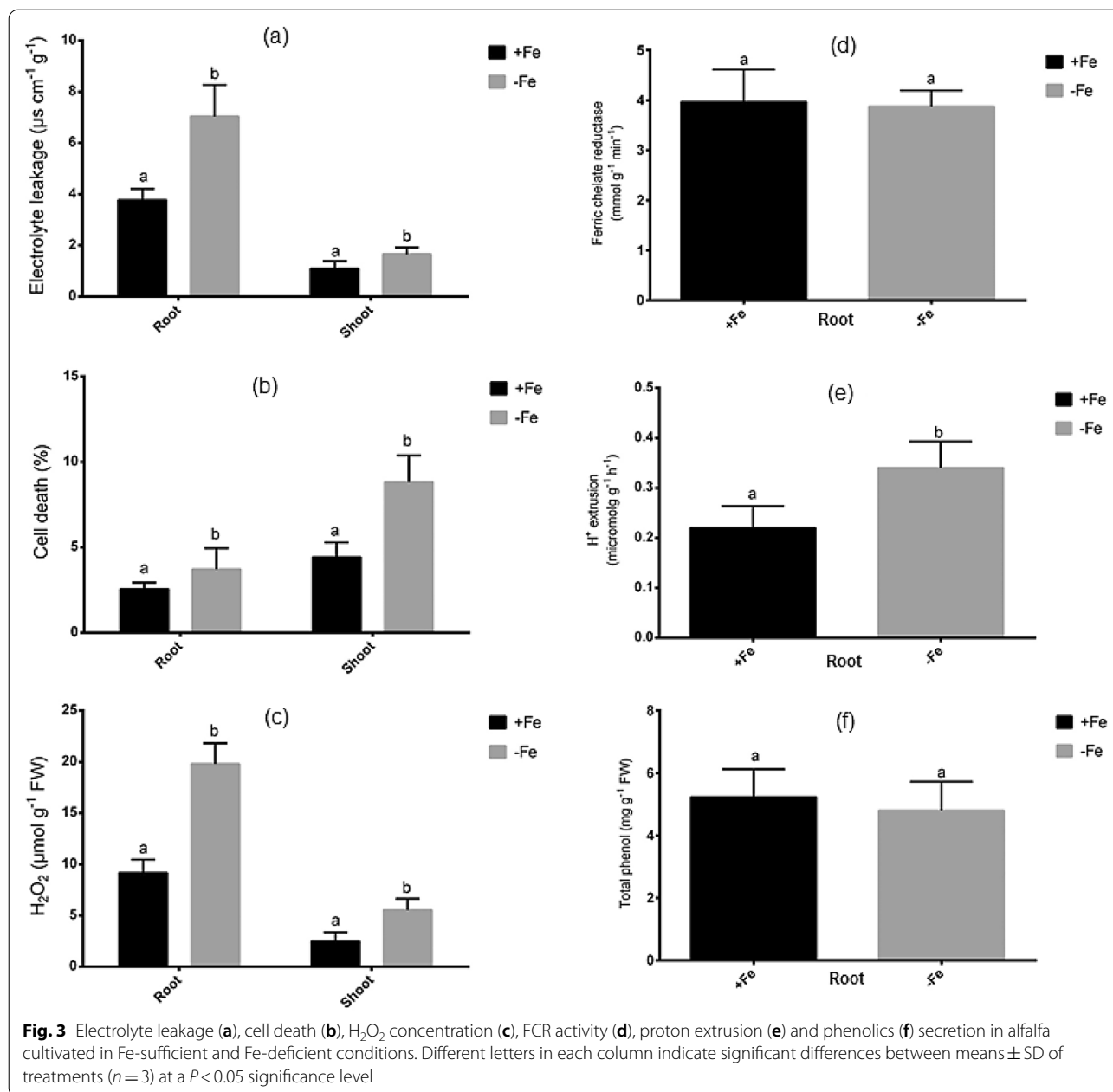


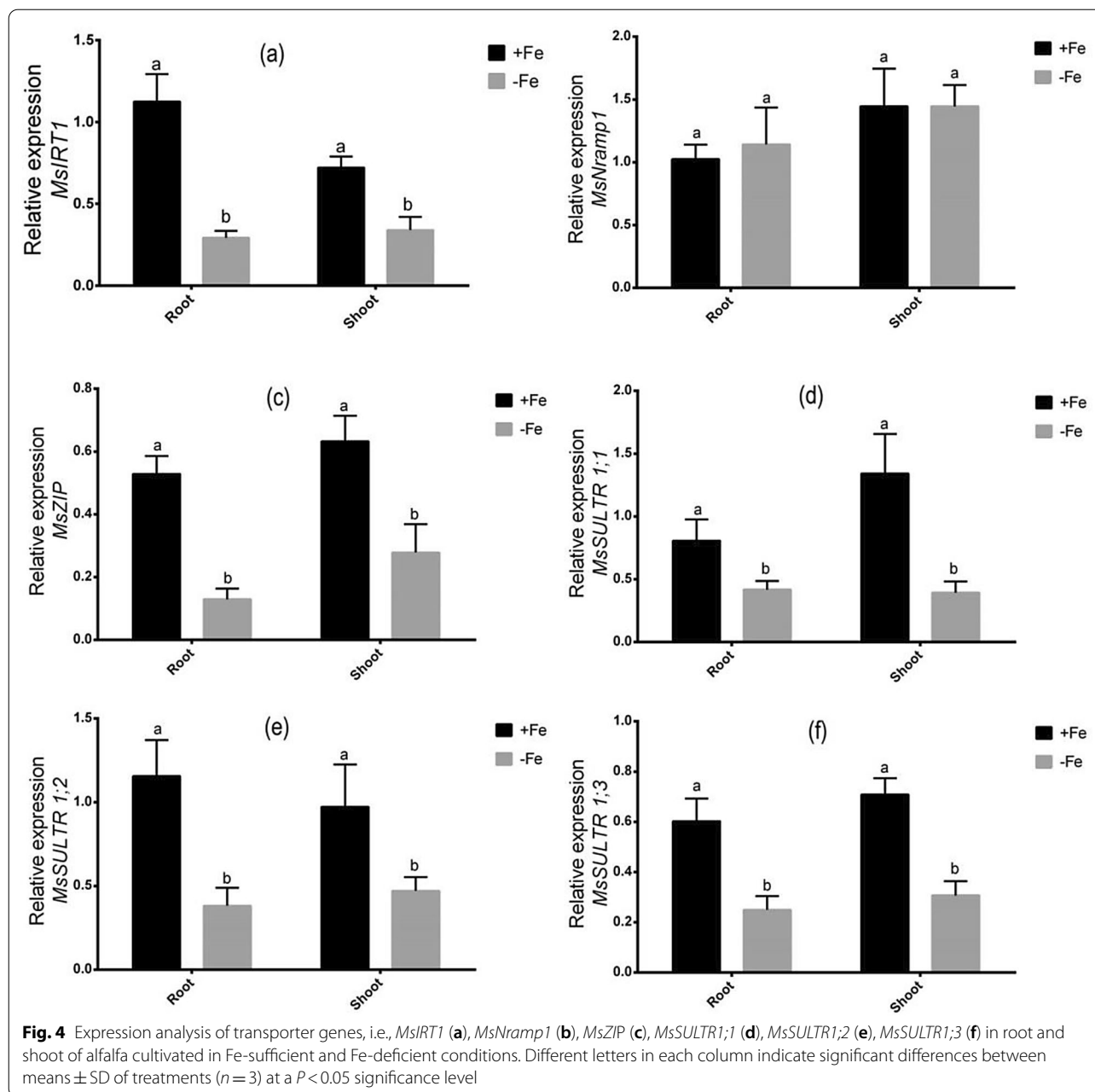
Table 1 Elemental concentrations (mg g⁻¹ DW) in root and shoot of alfalfa cultivated under + Fe and -Fe growth conditions

Elements	Root		Shoot	
	+Fe	-Fe	+Fe	-Fe
Fe	164 ± 15.2 ^a	97 ± 16.9 ^b	85 ± 12.1 ^a	41 ± 8.9 ^b
Zn	141 ± 34.0 ^a	64 ± 13.5 ^b	64 ± 10.2 ^a	33 ± 5.9 ^b
S	14,014 ± 202.2 ^a	10,613 ± 157.6 ^b	4567 ± 203.4 ^a	2145 ± 47.6 ^b
Ca	834 ± 176.2 ^a	511 ± 68.3 ^b	507 ± 48.7 ^a	497 ± 50.6 ^a

Data represent means ± SD (n = 3). Different letters indicate significant difference at P < 0.05 level

supports the diagnosis of Fe-deficiency symptoms and suggests the reduction in quantum yield efficiency in alfalfa in response to Fe shortage.

In this study, the relationship between quantum yield efficiency (Fv/Fm) and tissue Fe was further evaluated. The Fe concentration was severely decreased under Fe starvation in both root and shoot of alfalfa. Furthermore, the chlorophyll and PSII status clearly shows that Fe deficiency tends to inhibit alfalfa growth, but it is also closely related to photosynthetic kinetics. The Fe-deficient leaves are frequently linked to a reduction in PSII quantum

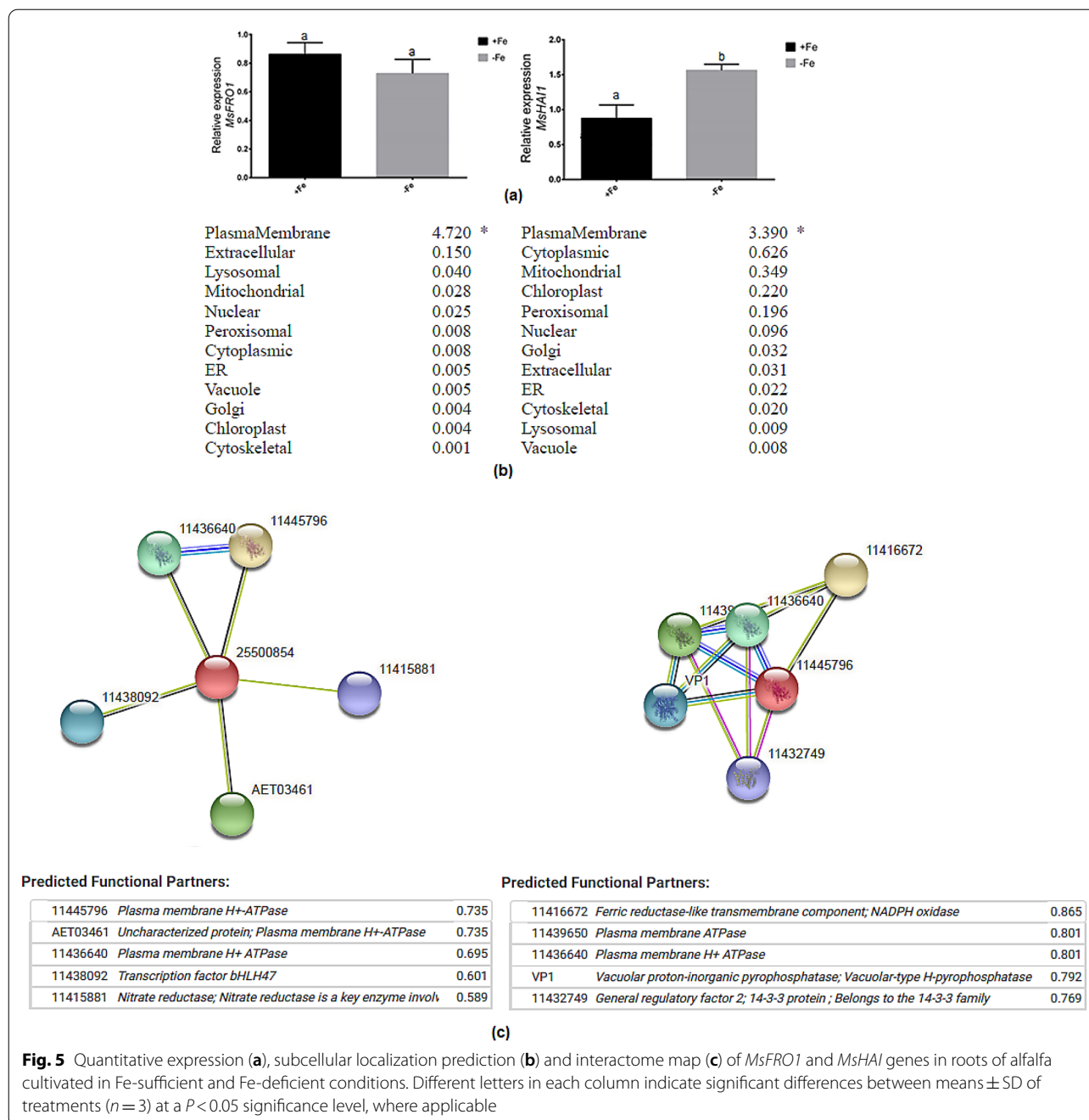


yield [39]. Another OJIP parameter, Pi_ABS, linked to the energy conservation efficiency index for photons absorbed by the PS-II antenna, also declined gradually in Fe-depleted alfalfa leaves. A chlorotic leaf is also strongly associated with PSII efficacy in plants with Fe deficiency, according to several studies [40–42]. However, this relationship can differ depending on the plant species, and mineral deficiency has been shown to negatively affect the redox state of PSII acceptors in sugar beet [43]. Furthermore, in Fe-deficient leaves, proteins linked to the reaction center and light-harvesting antenna normally

decrease [44]. Changes in PSII parameters in Fe-depleted alfalfa may be related to damage in the reaction center or various elements of the PSII system's energy transfer path, according to our findings. This message will help to reinforce awareness about how to protect alfalfa's photosynthetic apparatus from harm.

Changes in elemental concentration and transporter genes

This study revealed the interactions of Fe with a broad range of other nutrient elements in response to Fe-deficiency in alfalfa. In this study, the relationship between



photosynthesis efficiency and tissue Iron was further correlated. The Fe concentration was severely decreased under Fe starvation in both root and shoot of alfalfa. We also found that the *MsIRT1* gene significantly downregulated in root and shoot of alfalfa due to Fe deficiency, suggesting that this *IRT1* transporter is directly associated with the decreased Fe uptake and bioavailability in the rhizosphere along with its long-distance transport of Fe to the aerial part that eventually resulted in overall plant

growth and photosynthesis damages in alfalfa plants. The constitutive expression of *MsNramp1* in alfalfa suggests that alfalfa plants tend to absorb the available Fe through this transporter; however, this gene is not linked to the differential tolerance of alfalfa in response to Fe-deficiency in alfalfa plants. In response to Fe deficiency, a dual pattern of *IRT1* expression has been observed in plants [45, 46]. As a result, it is likely that the expression is highly dependent on the cultivar/species' genotypic

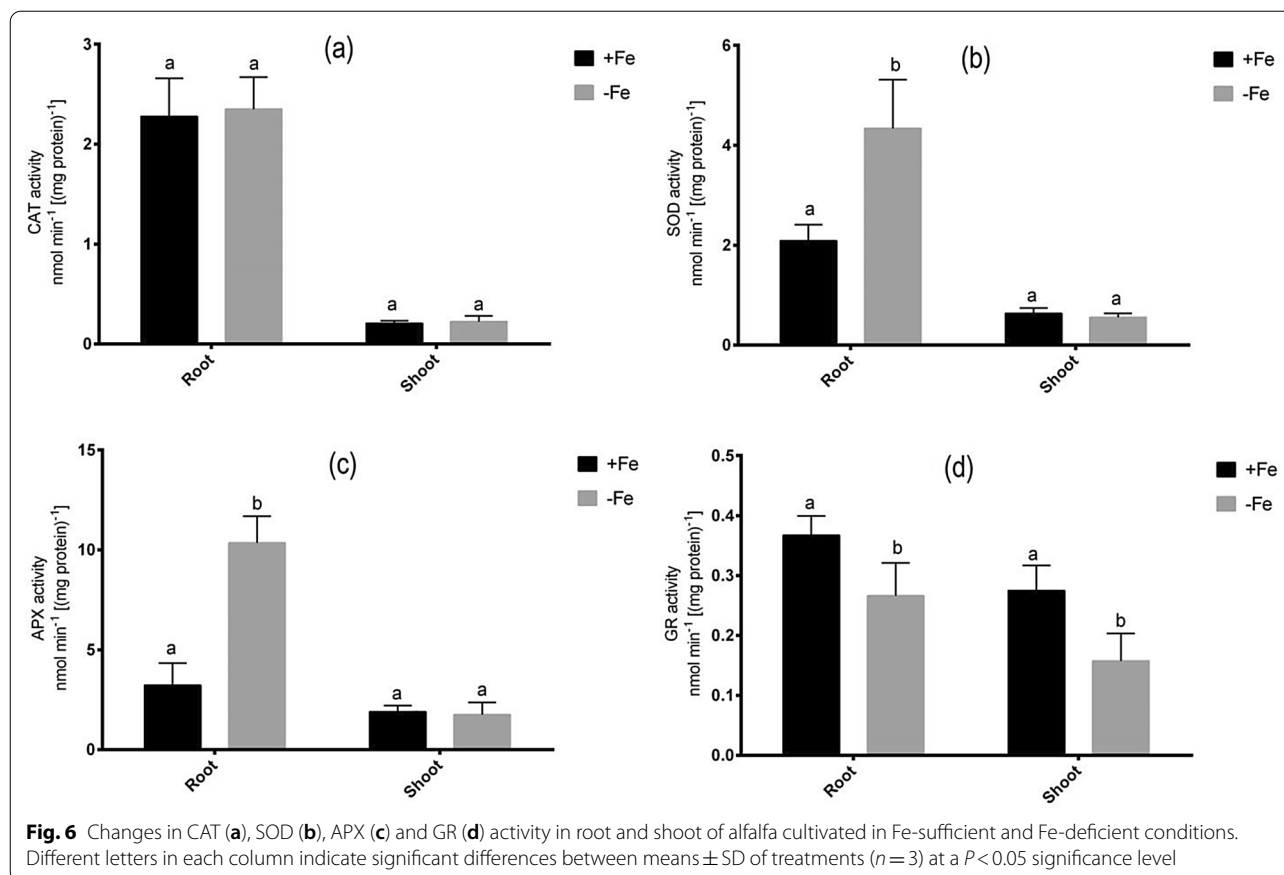


Table 2 S-metabolites ($\mu\text{g g}^{-1}$ FW) in root of alfalfa cultivated under + Fe and -Fe growth conditions

S-metabolites	Control	-Fe
Glutathione	4.1 ± 2.0^a	4.3 ± 1.1^a
Cysteine	2.3 ± 1.1^a	2.2 ± 0.88^a
Methionine	3.8 ± 0.9^a	3.9 ± 1.1^a

Data represent means \pm SD ($n = 3$). Different letters indicate significant difference at $P < 0.05$ level

context as well as the period of stress exposure to the plants. ZIP proteins can also play a role in Fe and Zn uptake and transport in plants [13, 14]. The decrease in Zn concentration and *MsZIP* expression in Fe-deficient alfalfa tissues is very consistent with this. In general, plants are induced to express ZIP genes when they are deficient in Zn, which promotes cell Zn influx and Zn movement between species, as well as when they are deficient in Fe or Mn [17, 47]. Our findings suggest that *MsZIP* is involved in, at least in part, Fe acquisition in alfalfa plants, or is fully dedicated to Zn uptake in alfalfa plants, or is highly interfering with the alfalfa plants' Fe status.

In contrast to previous research on Fe transporters [48], it was discovered that *IRT1* expression was induced in Fe-depleted tomatoes. However, the plants were sufficient with S status. To investigate the involvement of S in Fe nutrition, we found that S concentration and genes responsible for S uptake and transporters (*MsSULTR1;1*, *MsSULTR1;2* and *MsSULTR1;3*) substantially downregulated following Fe starvation in alfalfa. This reveals that Fe starvation severely hinders the S status of the plants that may also affect the Strategy I responses of alfalfa owing to Fe-deficiency. This evidence is in accordance with Fe-starved tomato in which S-deficiency for more than 10d limited the expression of the *IRT1* gene under Fe-deficiency [45]. It is also possible that cell damage may alter gene expression patterns [49]. The demand for Fe and S in the organelles for the biosynthesis of Fe-S clusters is a feedback signal that coordinates the absorption and reduction of both nutrients [19]. The activity of photosynthesis and RuBisCO activity was closely related to S status in rapeseed leaves [45]. Thus, it is evident that the S status is vital for Fe acquisition and transport in Fe-deficient plants. Not only Zn and S but the Ca level also dramatically dropped in Fe-deprived alfalfa, indicating

that Ca signaling is also a part of Fe homeostasis in alfalfa plants. Studies suggest that the CIPK23 complex of the Ca^{2+} channel is responsible for Fe and Zn transport in Arabidopsis. As a result, we believe that Fe deficiency-induced reduction of Fe is intimately linked to the status of other elements, especially Zn and S, resulting in overall stress sensitivity in alfalfa plants. Furthermore, the downregulation of *MsIRT1* and *MsZIP* genes, as well as the reduced expression of S transporters, are largely responsible for the decreased Fe uptake and subsequent translocation, which is consistent with the extreme chlorosis and PS-II damage seen in Fe-depleted alfalfa.

Changes in Strategy I responses

The major Strategy I responses to understand the status of these adaptive traits in Fe-deprived alfalfa plants have been assessed. We observed that FCR activity and its responsible *MsFRO1* gene were stable in the root of alfalfa, which seemed to be a response to withstand Fe-deficiency but was not substantially induced due to the lack of available Fe in the rhizosphere. Other plants have shown constitutive expression or upregulation of the *FRO1* gene, also in Fe-deficient plants [50, 51]. FCR has been linked to differential resistance to Fe deficiency in a variety of Strategy II plants [1, 52]. Our results build on these previous findings confirm that regulation of FCR activity is a significant issue associated with the inefficiency of alfalfa plants to maintain sufficient Fe in the root system.

In soil with a pH greater than 8.0, Fe becomes inaccessible to plants [1]. As a result, plants release H^+ into the rhizosphere to lower the pH [9, 51]. As evidenced by proton extrusion activity and *MsHAI* expression in alfalfa roots, this is a typical Strategy I response for Fe acquisition that has increased significantly. Other dicot plants have been shown to be involved in proton extrusion in Fe-depleted conditions [1, 53]. While proton extrusion can help alfalfa absorb Fe, this adaptive mechanism was not enough to control the overall Fe absorption system in Fe-deficient alfalfa. However, we did not observe any changes of the phenolic compounds in response to Fe-deficiency, suggesting that the magnitude or efficiency of phenolic compounds to withstand Fe-deficiency is genotype-dependent. However, root Fe reductase and phosphoenolpyruvate carboxylase activities, as well as acidification capacity, were higher in Fe-deficient plants' roots than in control plants' roots in a prior study on alfalfa [54]. Furthermore, overcoming Fe deficiency-induced responses in alfalfa plants is a complex process that may require cumulative biochemical and molecular induction of Strategy I responses. Furthermore, the phenolic compounds released by roots in Fe deficiency, which are responsible for Fe chelation and radical scavenging

[55, 56], do not appear to be involved in Fe homeostasis in alfalfa plants. The interaction network of a particular gene provides information about interactions that may influence plant control in response to specific stress. Our analysis reveals the involvement of several partner genes, such as plasma membrane H^+ -ATPase, transcription factor *bHLH47*, ferric reductase-like transmembrane component, vacuolar-type H-pyrophosphatase, and nitrate reductase genes, that may be attributed to Fe-efficiency mechanisms in alfalfa plants. Resequencing of genome variants can reveal valuable information about changes in alfalfa responses to Fe deficiency stress [57]. Overall, the findings of this interactome analysis may be crucial for functional genomics studies of Fe uptake and transport in alfalfa and related plant organisms.

Redox status and antioxidant properties

Plants starving with Fe are more prone to oxidative stress as Fe is a co-factor of many antioxidant enzymes. The CAT enzyme, which protects plants from active O_2 radicals, remained unchanged in Fe-starved alfalfa. However, SOD and APX activities remarkably enhanced only in roots of alfalfa, suggesting that alfalfa plants tend to counteract elevated ROS, although to a lesser extent. The rise in SOD and APX activity may mitigate the increased superoxide radicals Fe-deficient alfalfa roots. Still, the magnitude of functionality was not sufficient enough to perform a complete diminish of ROS in alfalfa. Several studies reveal the roles of SOD in protecting stress-induced oxidative damages [58, 59]. Evidence also reported on the association of low Fe availability and reduced peroxidase in plants [41]. The Fe-deficiency caused a decrease in alfalfa root and shoot, suggesting that this crucial antioxidant enzyme associated with the ascorbate–glutathione cycle seems to be inactive in which the decline of S status might play a role. The S-induced physiological benefits and antioxidant defense are often seen on Fe-deficient plants [9, 60]. In this study, none of the S-metabolites showed induction due to decreased Fe and S status of alfalfa plants under Fe deficiency. Mainly, glutathione was reported to be allied with the Fe-deficiency tolerances in Strategy I plants [1, 61]. Overall, the Fe-deficiency-induced antioxidant defense was partly induced, predominantly in roots, left the aerial part full of ROS, causing damages in growth and chloroplasts proteins in alfalfa.

Conclusions

The current research adds to our understanding of the mechanical basis for alfalfa plant responses to Fe deficiency. The Fe deprivation caused a severe reduction in alfalfa biomass, chlorophyll synthesis, photosynthesis efficiency, and cellular integrity. The results showed

that the Fe-deficiency not only reduced Fe concentration, but also severely affect the Zn, S, and Ca status in alfalfa plants. This physiological evidence was further supported by the downregulation of Fe and S transporters in Fe-starved alfalfa roots. The constitutive expression of FCR activity in roots suggests the key response in Fe-deficient alfalfa but sufficient induced under low Fe availability. Although proton extrusion, along with SOD and APX enzyme activities, was induced in roots, these did not withstand the Fe-deficiency symptoms and oxidative burst in alfalfa. Bioinformatics analysis further revealed the localization of *MsFRO1* and *MsHAI1* genes in the plasma membrane in addition to the interactome partnership predominantly with plasma membrane H⁺-ATPase, transcription factor *bHLH47*, and vacuolar-type H-pyrophosphatase. These findings add to our knowledge of alfalfa's Fe-starvation responses, which can be used to enhance alfalfa or other legume plants that are vulnerable to Fe deficiency.

Supplementary Information

The online version contains supplementary material available at <https://doi.org/10.1186/s40538-021-00235-6>.

Additional file 1: Table S1. List of primers used for qPCR.

Acknowledgements

We are very grateful to the Central Science Laboratory of the University of Rajshahi. The authors also extend their appreciation to the International Scientific Partnership Program ISPP at King Saud University for funding this research work through ISPP-128.

Authors' contributions

MAR performed qPCR and ICP-MS analysis. MBA and FA conducted bioinformatics analysis. KDA and NZ edited the manuscript. KL provided valuable advice during the research work. AHK prepared the draft manuscript and supervised the whole work. All authors read and approved the final manuscript.

Funding

The authors extend their appreciation to the International Scientific Partnership Program ISPP at King Saud University for partially funding this research work through ISPP-128.

Availability of data and materials

The data that support the findings of this study are in the article itself.

Declarations

Ethics approval and consent to participate

All authors approved the manuscript.

Consent for publication

All authors provided consent for publication.

Competing interests

We have no conflict of interest.

Author details

¹Grassland and Forage Division, National Institute of Animal Science, Rural Development Administration, Cheonan 31000, Republic of Korea. ²Biodiversity

Centre, Institut de Recherche en Biologie Végétale, Université de Montréal and Jardin Botanique de Montréal, Montréal, QC 22001, Canada. ³Department of Soil Sciences, College of Food and Agricultural Sciences, King Saud University, Riyadh 11451, Saudi Arabia. ⁴Institut de Recherche en Biologie Végétale (IRBV), University of Montreal, 4101 Sherbrooke Est, Montréal, QC H1X 2B2, Canada. ⁵Quebec Research and Development Centre, Agriculture and Agri-Food Canada, Quebec, QC, Canada. ⁶Molecular Plant Physiology Laboratory, Department of Botany, University of Rajshahi, Rajshahi 6205, Bangladesh.

Received: 22 April 2021 Accepted: 10 June 2021

Published online: 20 July 2021

References

- Kabir AH, Paltridge NG, Roessner U, Stangoulis JCR. Mechanisms associated with Fe-deficiency tolerance and signaling in shoots of *Pisum sativum*. *Physiol Plant*. 2013;147:381–95.
- Alcántara E, Romera FJ, Canete M, De la Guardia MD. Effects of bicarbonate and iron supply on Fe (III) reducing capacity of roots and leaf chlorosis of the susceptible peach rootstock "Nemaguard." *J Plant Nutr*. 2000;23:1607–17.
- Zhang X, Zhang D, Sun W, Wang T. The adaptive mechanism of plants to iron deficiency via iron uptake, transport, and homeostasis. *Int J Mol Sci*. 2019;20:2424.
- Lukes, P. et al. Special electromagnetic agents: from cold plasma to pulsed electromagnetic radiation. In: *Bioelectrics*. Springer; 2017. p. 109–154.
- Wang M-Y, Xia R-X, Hu L-M, Dong T, Wu Q-S. Arbuscular mycorrhizal fungi alleviate iron deficient chlorosis in *Poncirus trifoliata* L. Raf under calcium bicarbonate stress. *J Hort Sci Biotechnol*. 2007;82:776–80.
- Rodríguez-Celma J, Lin WD, Fu GM, Abadía J, López-Millán AF, Schmidt W. Mutually exclusive alterations in secondary metabolism are critical for the uptake of insoluble iron compounds by *Arabidopsis* and *Medicago truncatula*. *Plant Physiol*. 2013;162(3):1473–85.
- Jin CW, You GY, He YF, Tang C, Wu P, Zheng SJ. Iron deficiency-induced secretion of phenolics facilitates the reutilization of root apoplastic iron in red clover. *Plant Physiol*. 2007;144(1):278–85.
- Walker EL, Connolly EL. Time to pump iron: iron-deficiency-signaling mechanisms of higher plants. *Curr Opin Plant Biol*. 2008;11:530–5.
- Kabir AH, Rahman MM, Haider SA, Paul NK. Mechanisms associated with differential tolerance to Fe deficiency in okra (*Abelmoschus esculentus* Moench). *Environ Exp Bot*. 2015;112:16–26.
- Młodzińska E. Alteration of plasma membrane H⁺-ATPase in cucumber roots under different iron nutrition. *Acta Physiol Plant*. 2012;34:2125–33.
- Colangelo EP, Guerinot ML. The essential basic helix-loop-helix protein FIT1 is required for the iron deficiency response. *Plant Cell*. 2004;16:3400–12.
- Shen J, et al. Bactericidal effects against *S. aureus* and physicochemical properties of plasma activated water stored at different temperatures. *Sci Rep*. 2016;6:28505.
- Eckhardt U, Marques AM, Buckhout TJ. Two iron-regulated cation transporters from tomato complement metal uptake-deficient yeast mutants. *Plant Mol Biol*. 2001;45:437–48.
- Vert G, Briat J, Curie C. *Arabidopsis* IRT2 gene encodes a root-periphery iron transporter. *Plant J*. 2001;26:181–9.
- Korshunova YO, Eide D, Clark WG, Guerinot ML, Pakrasi HB. The IRT1 protein from *Arabidopsis thaliana* is a metal transporter with a broad substrate range. *Plant Mol Biol*. 1999;40:37–44.
- Chen H-M, Wang Y-M, Yang H-L, Zeng Q-Y, Liu Y-J. NRAMP1 promotes iron uptake at the late stage of iron deficiency in poplars. *Tree Physiol*. 2019;39:1235–50.
- Vert G, et al. IRT1, an *Arabidopsis* transporter essential for iron uptake from the soil and for plant growth. *Plant Cell*. 2002;14:1223–33.
- Burleigh SH, Kristensen BK, Bechmann IE. A plasma membrane zinc transporter from *Medicago truncatula* is up-regulated in roots by Zn fertilization, yet down-regulated by arbuscular mycorrhizal colonization. *Plant Mol Biol*. 2003;52:1077–88.
- Foieri I, Wirtz M, Hell R. Toward new perspectives on the interaction of iron and sulfur metabolism in plants. *Front Plant Sci*. 2013;4:357.

20. Cao M, et al. SULTR 3; 1 is a chloroplast-localized sulfate transporter in *Arabidopsis thaliana*. *Plant J.* 2013;73:607–16.
21. Takahashi H, Kopriva S, Giordano M, Saito K, Hell R. Sulfur assimilation in photosynthetic organisms: molecular functions and regulations of transporters and assimilatory enzymes. *Annu Rev Plant Biol.* 2011;62:157–84.
22. Wilkins KA, Matthus E, Swarbreck SM, Davies JM. Calcium-mediated abiotic stress signaling in roots. *Front Plant Sci.* 2016;7:1296.
23. Kudla J, et al. Advances and current challenges in calcium signaling. *New Phytol.* 2018;218:414–31.
24. Halliwell B. Reactive species and antioxidants. Redox biology is a fundamental theme of aerobic life. *Plant Physiol.* 2006;141:312–22.
25. Yang Y, et al. The combined effects of arbuscular mycorrhizal fungi (AMF) and lead (Pb) stress on Pb accumulation, plant growth parameters, photosynthesis, and antioxidant enzymes in *Robinia pseudoacacia* L. *PLoS ONE.* 2015;10:e0145726.
26. Ashraf M. Biotechnological approach of improving plant salt tolerance using antioxidants as markers. *Biotechnol Adv.* 2009;27:84–93.
27. Mittova V, Tal M, Volokita M, Guy M. Up-regulation of the leaf mitochondrial and peroxisomal antioxidative systems in response to salt-induced oxidative stress in the wild salt-tolerant tomato species *Lycopersicon pennellii*. *Plant Cell Environ.* 2003;26:845–56.
28. Kabir AH, et al. Genetic variation in Fe toxicity tolerance is associated with the regulation of translocation and chelation of iron along with antioxidant defence in shoots of rice. *Funct Plant Biol.* 2016;43:1070–81.
29. Hoagland DR, Arnon DI. The water-culture method for growing plants without soil. *Circ Calif Agric Exp Stn.* 1950;347.
30. Zhao D, Reddy KR, Kakani VG, Reddy VR. Nitrogen deficiency effects on plant growth, leaf photosynthesis, and hyperspectral reflectance properties of sorghum. *Eur J Agron.* 2005;22:391–403.
31. Lutts S, Kinet JM, Bouharmont J. NaCl-induced senescence in leaves of rice (*Oryza sativa* L.) cultivars differing in salinity resistance. *Ann Bot.* 1996;78:389–98.
32. Alexieva V, Sergiev I, Mapelli S, Karanov E. The effect of drought and ultraviolet radiation on growth and stress markers in pea and wheat. *Plant Cell Environ.* 2001;24:1337–44.
33. Kogure K, et al. Novel antioxidants isolated from plants of the genera *Ferula*, *Inula*, *Prangos* and *Rheum* collected in Uzbekistan. *Phytomedicine.* 2004;11:645–51.
34. Yu C, Chen Y, Lu C, Hwang J. Prediction of protein subcellular localization. *Proteins Struct Funct Bioinforma.* 2006;64:643–51.
35. Szklarczyk D, et al. STRING v11: protein–protein association networks with increased coverage, supporting functional discovery in genome-wide experimental datasets. *Nucleic Acids Res.* 2019;47:D607–13.
36. Misra NN, et al. Atmospheric pressure cold plasma (ACP) treatment of wheat flour. *Food Hydrocoll.* 2015;44:115–21.
37. Sun M, Zigman S. An improved spectrophotometric assay for superoxide dismutase based on epinephrine autoxidation. *Anal Biochem.* 1978;90:81–9.
38. Li G, Wang B, Tian Q, Wang T, Zhang WH. *Medicago truncatula* ecotypes A17 and R108 differed in their response to iron deficiency. *J Plant Physiol.* 2014;171(8):639–47.
39. Abadía J, Morales F, Abadía A. Photosystem II efficiency in low chlorophyll, iron-deficient leaves. *Plant Soil.* 1999;215:183–92.
40. Gogorcena Y, Molias N, Larbi A, Abadía J, Abadía A. Characterization of the responses of cork oak (*Quercus suber*) to iron deficiency. *Tree Physiol.* 2001;21:1335–40.
41. Donnini S, Castagna A, Guidi L, Zocchi G, Ranieri A. Leaf responses to reduced iron availability in two tomato genotypes: t3238 fer (iron efficient) and t3238 fer (iron inefficient). *J Plant Nutr.* 2003;26:2137–48.
42. Behera S, et al. Two spatially and temporally distinct Ca²⁺ signals convey *Arabidopsis thaliana* responses to K⁺ deficiency. *New Phytol.* 2017;213:739–50.
43. Belkhodja R, et al. Iron deficiency causes changes in chlorophyll fluorescence due to the reduction in the dark of the photosystem II acceptor side. *Photosynth Res.* 1998;56:265–76.
44. Devadasu ER, Madireddi SK, Nama S, Subramanyam R. Iron deficiency cause changes in photochemistry, thylakoid organization, and accumulation of photosystem II proteins in *Chlamydomonas reinhardtii*. *Photosynth Res.* 2016;130:469–78.
45. Muneer S, et al. Involvement of sulphur nutrition in modulating iron deficiency responses in photosynthetic organelles of oilseed rape (*Brassica napus* L.). *Photosynth Res.* 2014;119:319–29.
46. Connolly EL, Fett JP, Guerinot ML. Expression of the IRT1 metal transporter is controlled by metals at the levels of transcript and protein accumulation. *Plant Cell.* 2002;14:1347–57.
47. Ramesh SA, Shin R, Eide DJ, Schachtman DP. Differential metal selectivity and gene expression of two zinc transporters from rice. *Plant Physiol.* 2003;133:126–34.
48. Li L, Cheng X, Ling H-Q. Isolation and characterization of Fe (III)-chelate reductase gene LeFRO1 in tomato. *Plant Mol Biol.* 2004;54:125–36.
49. Henriques R, et al. Knock-out of *Arabidopsis* metal transporter gene IRT1 results in iron deficiency accompanied by cell differentiation defects. *Plant Mol Biol.* 2002;50:587–97.
50. Jelali N, Dell'orto M, Abdely C, Gharsalli M, Zocchi G. Changes of metabolic responses to direct and induced Fe deficiency of two *Pisum sativum* cultivars. *Environ Exp Bot.* 2010;68:238–46.
51. Bouman BAM, Humphreys E, Tuong TP, Barker R. Rice and water. *Adv Agron.* 2007;92:187–237.
52. Waters BM, Blevins DG, Eide DJ. Characterization of FRO1, a pea ferric-chelate reductase involved in root iron acquisition. *Plant Physiol.* 2002;129:85–94.
53. Santi S, Schmidt W. Dissecting iron deficiency-induced proton extrusion in *Arabidopsis* roots. *New Phytol.* 2009;183:1072–84.
54. Andaluz S, Rodríguez-Celma J, Abadía A, Abadía J, López-Millán AF. Time course induction of several key enzymes in *Medicago truncatula* roots in response to Fe deficiency. *Plant Physiol Biochem PPB.* 2009;47(11–12):1082–8.
55. Curie C, Briat J-F. Iron transport and signaling in plants. *Annu Rev Plant Biol.* 2003;54:183–206.
56. Blum U, Staman KL, Flint LJ, Shafer SR. Induction and/or selection of phenolic acid-utilizing bulk-soil and rhizosphere bacteria and their influence on phenolic acid phytotoxicity. *J Chem Ecol.* 2000;26:2059–78.
57. Wang TZ, Tian QY, Wang BL, Zhao MG, Zhang WH. Genome variations account for different response to three mineral elements between *Medicago truncatula* ecotypes Jemalong A17 and R108. *BMC Plant Biol.* 2014;14:122.
58. Sun B, et al. Protective effect of nitric oxide on iron deficiency-induced oxidative stress in maize (*Zea mays*). *J Plant Physiol.* 2007;164:536–43.
59. Molassiotis A, Tanou G, Diamantidis G, Patakas A, Therios I. Effects of 4-month Fe deficiency exposure on Fe reduction mechanism, photosynthetic gas exchange, chlorophyll fluorescence and antioxidant defense in two peach rootstocks differing in Fe deficiency tolerance. *J Plant Physiol.* 2006;163:176–85.
60. Zuchi S, Cesco S, Varanini Z, Pinton R, Astolfi S. Sulphur deprivation limits Fe-deficiency responses in tomato plants. *Planta.* 2009;230:85–94.
61. Zaharieva TB, Gogorcena Y, Abadía J. Dynamics of metabolic responses to iron deficiency in sugar beet roots. *Plant Sci.* 2004;166:1045–50.

Publisher's Note

Springer Nature remains neutral with regard to jurisdictional claims in published maps and institutional affiliations.